Low Energy Neutral Atoms in the Magnetosphere

T. E. Moore,[1] M. R. Collier,[1] J. L. Burch,[2] D. J. Chornay,[1,3] S. A. Fuselier,[4] A. G. Ghielmetti,[4] B. L. Giles,[1] D. C. Hamilton,[3] F. A. Herrero,[1] J. W. Keller,[1] K. W. Ogilvie,[1] B. L. Peko,[5] J. M. Quinn,[6] T. M. Stephen,[5] G. R. Wilson,[7] P. Wurz,[8]

Abstract. We report observations of low energy neutral atoms from the solar wind and the ionosphere, obtained by the Low Energy Neutral Atom (LENA) Imager on the IMAGE spacecraft. The LENA Imager detects and images LENAs arriving at the spacecraft from within a 90° field of view (8°x8° pixels), swept through 360° every two minutes by spacecraft spin. Neutral atoms arriving at the sensor are converted to negative ions by a conversion surface. The resulting negative ions are separated in energy (3 bins, 10 - 250 eV) and arrival direction (±45°). They are then accelerated, detected, and time-of-flight mass analyzed as they pass through a thin foil and strike an image plane detector. The solar wind and the ionosphere both emit measurable neutral atom fluxes, the latter responding rapidly to to variations of the former.

Background

Geospace contains a mixture of low-density gases and plasmas of both solar and terrestrial origin. The terrestrial gas and ionospheric plasma are at a base temperature $\sim$ 1000-3000 K, depending on solar EUV flux. Solar plasma arrives at Earth's magnetosphere, after passing through a bow shock, at up to $\sim 3 \times 10^6$ K. Auroral processes raise ionospheric topside plasma temperatures to $\sim 10^5 - 3 \times 10^6$ K. ENA are produced in volumes where energetic ions and relatively cold gas coexist and undergo charge exchange [*Gruntman,* 1994]. Low energy ENA are defined by the technique required for their observation. Unlike medium and high energy neutral atoms, those with kinetic energy below 1 keV cannot penetrate the thinnest foils used, via secondary electron emission, to detect charge-free particles [*Wurz,* 1990].

The LENA Imager on IMAGE [*Moore et al.,* 2000] implements a new capability to observe LENA in the energy range extending from that of arriving solar wind ions ($\sim$ 0.5 to 4 keV) to that of ions escaping the ionosphere via auroral processes ($\sim$ 10eV - 3 keV). A charge-exchanging conversion surface consisting of volatile adsorbates is used to convert a fraction of the incoming LENA ($< 1\%$) to negatively charged ions of the same species. The conversion process is accompanied by energy loss and angular scattering, which limit achievable resolution. The converted ions are distributed around the direction of specular reflection from the conversion surface with a FWHM of $\sim 25°$, and around an energy of $\sim$0.60 of incident energy, with a FWHM of 30%. Sputtering of conversion surface atoms is an important process for atoms above the nominal LENA energy range (>300 eV). This yields negative ions at energies much lower than the incident neutral energy, which are then analyzed by the system as if they were converted incident neutrals with low energies.

The LENA Imager aperture contains a collimator and charged particle rejector that suppresses charged particle entry below ~50-100 keV. The LENA field of view spans ±45° in polar angle from the direction radially outward from the cylindrical IMAGE spacecraft. The spacecraft spin vector is anti-aligned with the orbital angular momentum vector (reverse cartwheel mode), and the period is 2.0 minutes.

Activation of the LENA Imager was completed on 3-5 May 2000. It has since observed a range of solar and geomagnetic conditions, including a number of coronal mass ejections and geospace storms. The IMAGE orbit has its apogee at $\sim 8R_E$ geocentric in the northern hemisphere, and perigee at ~1000 km altitude in the southern hemisphere, with an inclination of 89.5°, right ascension of ascending node of 12.5°, and argument of perigee initially 40°, increasing with precession. The apogee was initially near the noon-midnight meridian and has evolved seasonally.

In the next section, we illustrate the types of LENA populations that have been observed to date and their variations. In subsequent sections, we discuss and interpret the data indicating a LENA component originating in the solar wind, and another originating in acceleration and outflow of ionospheric ions.

Observations

Quiet Time LENA Environment

Plate 1A

Plate 1A is a spin spectrogram (collapsed in polar angle relative to the spin axis), illustrating the LENA environment during magnetically-quiet conditions. The x-axis is UT; the y-axis is spin angle (increasing with time) relative to nadir; and the color or z-axis is the rate of events registering a measured time-of-flight. The pair of light lines indicates the angular extent of the Earth as viewed from the spacecraft. During the bulk of this period while the spacecraft is near apogee and north of the ecliptic plane, the view is sunward for positive spin angles and tailward for negative spin angles. The period includes one uninterrupted apogee pass and two perigee passes (during which the view is rapidly changing and generally opposite to that described above). Ephemeris data at the bottom of the plot document the orbital orientation, from ~09-21 hrs MLT, with apogee in the dayside northern hemisphere.

The data include prominent radiation belt features that are nearly isotropic in spin angle. This feature is seen as the spacecraft passes through the equator on both down-leg (e.g. 0700-0800) and up-leg (~0720) portions of the orbit. The up-leg feature is much narrower in time owing to the orbit tilt, causing the up-leg to pass more rapidly through the inner radiation belts. The time-of-flight response to these events is essentially flat. These events are most likely caused by accidental coincidences between random events produced on both start and stop detectors by penetrating MeV electrons or secondary X-rays. Although recognizable in the spectrograms, these features are not so readily subtracted as background owing to their variability from pass to pass. This response is somewhat greater than expected from the structural design of the LENA instrument, which provides shielding that exceeds 4.5mm of Al in all directions from the MCP detector systems.

The quiet time data also include a feature with peak response when the LENA field of view points nearest to the sun, sweeping rapidly through perigees across the reference nadir direction, where the LENA imager field of view contains the Earth. This feature, the width of which in spin angle is essentially the width of the LENA response function (8°), was initially interpreted as a response to solar EUV, which had been observed in laboratory testing. EUV response is believed to result from photoelectron generation, most likely from the conversion surface, yielding dissociative attachment of photoelectrons to residual gas molecules near the surface; or direct photo-desorption of negative ions. Residual gas atom photoionization can also lead to negative ion production after impact of positive ions on the negatively charged surface. The negative ions masquerade as incident neutrals of very low energy. Such a response is expected to be proportional to the residual gas pressure. Based on pumpdown rates observed in thermal vacuum testing, the pressure after weeks on orbit is anticipated to be much lower ($\leq 10^{-8}$ torr) than in laboratory testing ($\sim 10^{-6}$ torr). Energy analysis of the solar signal suggests that at most 30-40% of it consists of very low energy neutrals consistent with the EUV excitation. Moreover, the majority of the signal registered as O rather than H. A reasonable interpretation for this is that this signal was produced by incident H atoms with energies greater than several hundred eV. These were shown in laboratory testing to produce O^- from sputtering of the adsorbates making up the active conversion surface. As discussed further below, we therefore interpret the solar signal as a mixture of EUV response and LENAs from the solar wind, observed from inside the magnetosphere, with the latter believed dominant.

Finally, the quiet pass spectrogram shows the brightest quiet time LENA signal from the direction of the Earth during perigee passes. Comparing the perigee passes in Plate 1, it is apparent that this signal varies from pass to pass. At times this signal is weak or absent. Plate 2 illustrates this signal in the form of image snapshots selected from the perigee pass near 0900 UT in Plate 1. The solar signal also appears in this series of images and is nearly occulted by the Earth at the end of the sequence. The greatest non-solar fluxes originate from the Earth below the spacecraft, and/or from the direction in which the spacecraft is travelling. This signal is believed to represent LENA outflow from the auroral ionosphere, at velocities comparable to or exceeding that of the spacecraft.

Plate 2

Active Period LENA Environment

Plate 1B is also a spin spectrogram, illustrating LENA features observed on 8 June 2000, including the period when a coronal mass ejection (CME) passed the Earth, resulting in a significant geomagnetic disturbance over the ensuing days. In Plate 1B, the solar signal trace is significantly dimmer than in Plate 1A. This owes to the increasing solar zenith angle relative to the IMAGE spin axis, causing the direct solar signal to move beyond the Imager field of view on or about 26 May 2000. The dimmer remaining solar signal, at about ∼45° in width, is significantly broader in spin angle than in Plate 1A. A brightening of the solar signal trace occurs at about 09:15 UT, very near the time the CME's leading shock reached the Earth. This brightening of the solar signal, in coincidence with the arrival of the CME ejecta, is incompatible with an exclusive EUV signal. We examined the 0.1-50 nm EUV flux measured on board the solar and heliospheric observer (SOHO) [*Judge et al.,* 1998] and no corresponding brightening of the sun's EUV emissions occurs on 8 June. In fact, the envelope of all variations on 8 June is limited to approximately 3%. There had been ∼50% spikes on the prior two days, but these did not produce significant brightenings of the LENA sun signal at those times.

Plate 3 shows individual images from selected times during this pass. The first image shows the total LENA flux for a one hour integration just prior to CME arrival at 0915UT. Here the perspective is from several R_E above the ecliptic plane, looking generally down on the dayside equatorial region. The main feature of interest in Plate 3A is the flux from the direction of the sun in spin angle, but near the center of the polar angle field of view. Weak emissions can be seen to emanate from the region near and around the Earth as well. The fact that the solar signal is roughly centered in the polar field of view suggests that the source of solar LENA signal is actually within the magnetosheath around 10-11 MLT, toward which the instrument is viewing when its FOV fan views most nearly toward the sun.

Plate 3

Plate 3B shows a similar one hour integration just after CME arrival. It indicates an increase in the total solar LENA emissions by a factor of ≥ 2, and a larger increase of the emissions from the regions near and around the Earth. These emissions are peaked in the Earthward sector, but also extend well away from the Earth, especially in the northward/tailward direction. Plate 3C is one carefully selected snapshot from within the 29 spin accumulation of image B. It shows that at one point (about 35 minutes after CME arrival), the Earth sector emission was much brighter than the sun signal (discussed further below).

Plate 3D shows a perigee pass perspective of the south polar regions, showing increased LENA emissions from the Earth at close range. These perigee fluxes are somewhat more intense and extended than in the quiet time case shown in Plates 1A and 2, although this appearance is exaggerated by a higher detector gain setting during the active event (discussed further below).

Figure 1

Figure 1 shows, for the CME arrival on 8 June, 2000, the LENA total atom rate summed over energy and over polar angle within spacecraft spin sectors corresponding to the Sun (left hand y-axis) and Earth (right hand y-axis). At shock passage, there was an enhancement in both the Sun and Earth directions. About 35 minutes later, there was a second and greater brightening from the Earth direction [*Fuselier et al.,* 2001], as was also illustrated in Plate 3C.

Discussion

Based on Figure 1, the total event rate from the Sun sector increased from about 2.0 cts/sec to about 5.5 cts/sec during the CME enhancement. At solar wind energies around 1keV, LENA's neutral hydrogen effective area was measured (including sputtering) at about $6.4 \times 10^{-5} cm^2$, yielding an integral flux of about $9 \times 10^4 cm^{-2} s^{-1}$. After the CME arrived, the solar wind flux was $1 \times 10^9 cm^{-2} s^{-1}$ ($12 cm^{-3}$ density and 800 km/s speed) yielding a flux ratio of neutrals to solar wind of $0.3 - 1 \times 10^{-4}$ during the CME-enhanced solar wind period. The uncertainty results from uncertainty in the energy of the observed LENAs, which reach 4 keV during the high speed solar wind intervals after shock passage in the event reported here, well beyond the 1keV upper energy to which LENA was calibrated.

A coincident CME and EUV enhancement being exceedingly unlikely and unobserved [*Collier et al.,* 2001], we interpret the CME enhancement from the solar direction as LENA originating from the solar wind. There are several potentially important interplanetary sources of LENA. These include: i) solar neutral atoms carried from the corona with the solar wind, ii) charge exchange with interstellar gas penetrating the solar system from the local interstellar medium, iii) charge exchange with outgassing from interplanetary dust and iv) charge exchange with the Earth's geocorona, which has a density comparable to that of the solar wind near the magnetopause [*Gruntman,* 1994]. The solar wind neutral flux inferred there is similar to that derived here. The enhancement of solar LENA reported here apparently originates from directions more than 45° from the sun in the sky, so magnetosheath emissions are evidently important. Results of modelling of magnetosheath emissions, supporting our interpretation, are reported elsewhere [*Collier et al.,* 2001].

The LENA total event rate from the earth sector reached a peak of nearly 10 cts/sec, during a burst delayed by about 35 minutes from the shock arrival. These events most likely are produced by O atoms with energies near 35 eV (velocity about 21 km/s), accelerated within a few minutes of shock arrival. This is consistent with the known energy of maximal ionspheric ion outflow flux [*Yau and Lockwood,* 1990]. For oxygen at this energy, the effective area is $\sim 6.4 \times 10^{-6} cm^2$, yielding integral flux from the Earth sector that peaks near $1.7 \times 10^6 cm^{-2} s^{-1}$.

The LENA directional flux from the Earth sector observed during perigee passes is comparable to or greater than the solar signal, more widespread in angle, and includes a rammed component that must be of very low energy ($\leq$5 eV). Quiet time fluxes for polar outflows, as in plate 2, reach $3s^{-1}pixel^{-1}$. On 25 May 2000, the imager operated with reduced detector gain, such that its effective area for O was reduced by a factor of 4 relative to nominal, to $1.6 \times 10^{-6}cm^2$, while pixel solid angle is 0.020 sr. Thus peak directional fluxes reached up to $0.95 \times 10^8 cm^{-2}sr^{-1}s^{-1}$. During the perigee after the CME arrival on 8 June 00, as shown in plate 3, O event rates reach $30s^{-1}pixel^{-1}$. However, the MCP gains were nominal at this time, so the effective area for O was $6.4 \times 10^{-6}cm^2$. The corresponding directional fluxes reach up to $2.4 \times 10^8 cm^{-2}sr^{-1}s^{-1}$.

The enhancements from the Earth direction are interpreted as neutral atom emission from the Earth's ionosphere and other extended plasma regions near the Earth, resulting from the shock's interaction with geospace. Solar EUV energy is continuously dissipated in the sunlit atmosphere, creating the ionosphere and plasmasphere, and widespread thermal light ion outflows of H^+ and He^+ ions throughout the high latitude regions. In addition, auroral dissipation of solar wind energy produces escaping outflows of energized light and heavy ions, emanating from the auroral zones. Escape fluxes of H^+ have been observed to locally approach $10^9 cm^{-2}s^{-1}$, while escape fluxes of O^+ are known to approach $10^{10} cm^{-2}s^{-1}$ [*Yau and Lockwood,* 1990; *Pollock et al.,* 1990]. As these energized outflows pass through the thermosphere and geocorona, they are converted into LENA escape according to the relevant densities and cross sections. The largest fluxes of ion outflow stem from heating transverse to the local magnetic field, but parallel acceleration becomes prominent at higher altitudes.

The emission of ionospheric LENA varies in response to solar wind disturbances such as CMEs, reflecting variations of ionospheric heating and outflow, and this response is more immediate than could be established with in situ spacecraft measurements [*Moore et al.,* 1999]. The observed diffuseness of the LENA emissions is likely a result of the broad angular distribution and low energy of accelerated ions in LENA source regions. Additional modeling of these processes will be required for their full interpretation.

Conclusions

Using a new kind of instrument sensitive to low energy neutral atoms, we have shown that the magnetosphere contains fluxes of such neutral atoms originating from both the solar wind and the ionosphere of the Earth.

We found that a flux of LENA originates from the solar wind and may be a useful monitor of the solar wind flux inside the magnetosphere, from which the direct solar wind is excluded. Modeling and long term data studies designed to discriminate among possible sources identified above will be the subject of future publications and studies over time as the Earth samples a changing environment of interstellar gases. More comprehensive study of solar LENAs is likely to open up new opportunities for remotely sensing their source environments.

We also found that LENA are emitted directly from the Earth's ionosphere with speeds comparable to and exceeding the escape speeds or satellite speeds. In the past, auroral zone ion outflows could only be sampled locally by *in situ* spacecraft, at best twice per few-hour orbit. The observations reported here indicate that the outflow response to solar wind variations (a CME shock) is instantaneous to within fast neutral atom travel times (10's of minutes), and that they offer a useful means of remote sensing regions of plasma heating and acceleration in the ionosphere.

Acknowledgments.
The authors are indebted for the creativity and dedication of the engineering and technical staffs of Goddard Space Flight Center, Lockheed Martin Advanced Technology Center, University of Maryland, University of Denver, the University of Bern, the University of New Hampshire, and the Southwest Research Institute.

References

Collier, M. R, et al., Observations of Neutral Atoms from the Solar Wind, J. Geophys. Res., in press, 2001.

S. A. Fuselier, et al., Ion outflow observed by IMAGE: Implications for source regions and heating mechanisms, Geophys. Res. Lett., this issue, 2001.

Gruntman, M.A. Neutral solar wind properties: Advance warning of major geomagnetic storms, J. Geophys. Res., 99, 19,213-19,227, 1994.

Judge, D.L, et al., First Solar EUV Irradiances Obtained from SOHO by the SEM, Solar Physics 177, 161-173, 1998.

Moore, T. E., et al., The Low Energy Neutral Atom Imager for IMAGE, Space Sci. Revs., 91(1-2,) p.155, 2000.

Moore, T. E., et al., Ionospheric mass ejection in response to a CME, Geophys. Res. Lett., 26(15), pp. 2339-2342, 1999.

Pollock, C. J., et al., A Survey of Upwelling Ion Event Characteristics, J. Geophys. Res. 95, 18969, 1990.

P. Wurz, Detection of Energetic Neutral Particles, in *The Outer Heliosphere: Beyond the Planets,* edited by K. Scherer et al., Copernicus Gesellschaft e.V., Katlenburg-Lindau, Germany, pp. 251-288 2000.

Yau, A. W., and M. Lockwood, Vertical ion flow in the polar ionosphere, Modeling Magnetospheric Plasma Geophys. Monogr. Ser., vol 44, edited by T. E. Moore, and J. H Waite, Jr., AGU, Washington, D. C., p.229, 1988.

T. E. Moore, Code 690, NASA Goddard Space Flight Center, Greenbelt, MD 20771 USA, e-mail: thomas.e.moore@gsfc.nasa.gov

(Received September 28, 2000; accepted November 22, 2000.)

---

[1] NASA Goddard Space Flight Center, Greenbelt, MD
[2] Southwest Research Institute, San Antonio, TX
[3] Department of Physics, University of MD, College Park
[4] Lockheed Martin ATC, Palo Alto, California
[5] Department of Physics, University of Denver
[6] Institute for EOS, University of New Hampshire, Durham
[7] Mission Research Corporation, Nashua, New Hampshire
[8] Physikalisches Institut, University of Bern, Switzerland

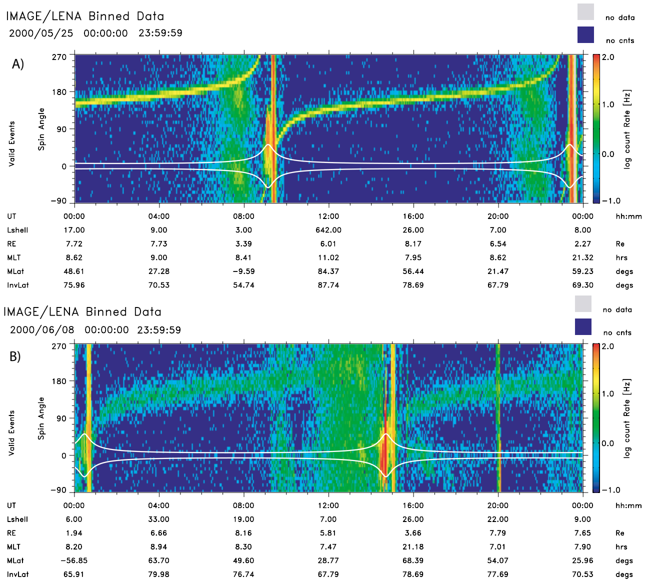

Plate 1. LENA total atoms (coincidence) spin spectrogram for A) the period of 25 May 2000, and B) for the CME event of 8 June 2000. Spin angle increases with time, with reference (0) to the nadir view. White lines indicate the limbs of the Earth.

Plate 1. LENA total atoms (coincidence) spin spectrogram for A) the period of 25 May 2000, and B) for the CME event of 8 June 2000. Spin angle increases with time, with reference (0) to the nadir view. White lines indicate the limbs of the Earth.

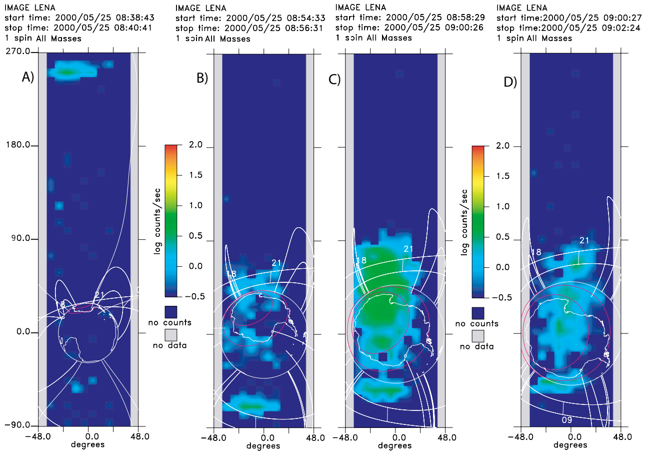

Plate 2. LENA image sequence for 25 May 2000; A) during downleg just past descending node, sun at top; B) approaching passage over the south polar regions, sun at lower left; C) passing over the Antarctica; and D) near perigee, with sun near occultation. Each image contains the Earth with continents, nominal auroral oval in red, and 3 and 6.6 R$_E$ magnetic field lines at the indicated magnetic local times.

Plate 2. LENA image sequence for 25 May 2000; A) during downleg just past descending node, sun at top; B) approaching passage over the south polar regions, sun at lower left; C) passing over the Antarctica; and D) near perigee, with sun near occultation. Each image contains the Earth with continents, nominal auroral oval in red, and 3 and 6.6 R$_E$ magnetic field lines at the indicated magnetic local times.

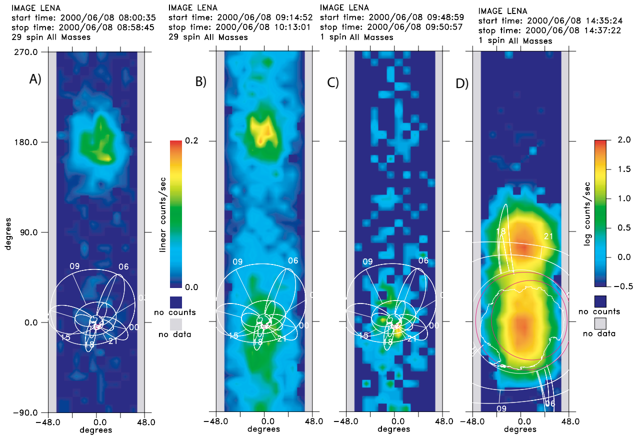

Plate 3. LENA image sequence for 8 June 2000; A) hour average before CME arrival at 0915; B) hour average after CME arrival; C) snapshot 35 min after CME arrival ; D) during passage over the south polar regions near perigee. Panels A, B, C have linear scaling (color bar C 10x higher than for A, B), whereas D) is logarithmic.

Plate 3. LENA image sequence for 8 June 2000; A) hour average before CME arrival at 0915; B) hour average after CME arrival; C) snapshot 35 min after CME arrival ; D) during passage over the south polar regions near perigee. Panels A, B, C have linear scaling (color bar C 10x higher than for A, B), whereas D) is logarithmic.

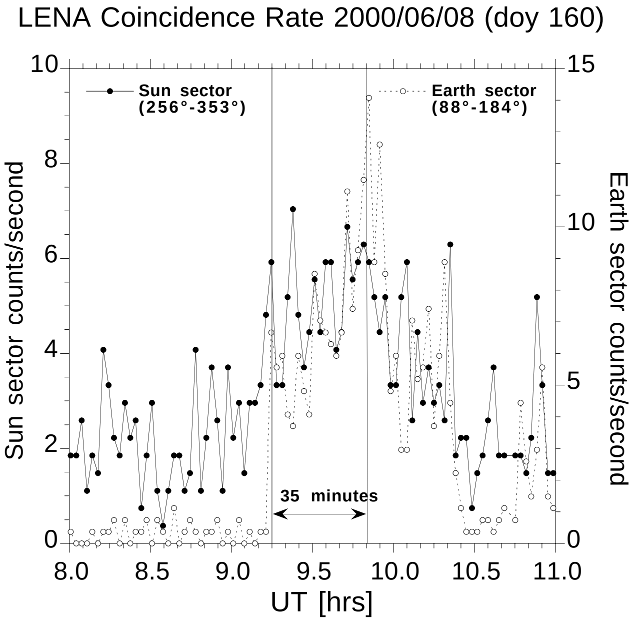

Figure 1. LENA total atom rates (single spin, 120 sec accumulations) from the sun sector (left y axis) and from the Earth sector (right y axis) vs. time for the 8 June 2000 CME event.

Figure 1. LENA total atom rates (single spin, 120 sec accumulations) from the sun sector (left y axis) and from the Earth sector (right y axis) vs. time for the 8 June 2000 CME event.

10

MOORE ET AL.: LOW ENERGY NEUTRAL ATOMS IN THE MAGNETOSPHERE

MOORE ET AL.: LOW ENERGY NEUTRAL ATOMS IN THE MAGNETOSPHERE

MOORE ET AL.: LOW ENERGY NEUTRAL ATOMS IN THE MAGNETOSPHERE

MOORE ET AL.: LOW ENERGY NEUTRAL ATOMS IN THE MAGNETOSPHERE

MOORE ET AL.: LOW ENERGY NEUTRAL ATOMS IN THE MAGNETOSPHERE

MOORE ET AL.: LOW ENERGY NEUTRAL ATOMS IN THE MAGNETOSPHERE

MOORE ET AL.: LOW ENERGY NEUTRAL ATOMS IN THE MAGNETOSPHERE

MOORE ET AL.: LOW ENERGY NEUTRAL ATOMS IN THE MAGNETOSPHERE

MOORE ET AL.: LOW ENERGY NEUTRAL ATOMS IN THE MAGNETOSPHERE

MOORE ET AL.: LOW ENERGY NEUTRAL ATOMS IN THE MAGNETOSPHERE

MOORE ET AL.: LOW ENERGY NEUTRAL ATOMS IN THE MAGNETOSPHERE

MOORE ET AL.: LOW ENERGY NEUTRAL ATOMS IN THE MAGNETOSPHERE

MOORE ET AL.: LOW ENERGY NEUTRAL ATOMS IN THE MAGNETOSPHERE

MOORE ET AL.: LOW ENERGY NEUTRAL ATOMS IN THE MAGNETOSPHERE

MOORE ET AL.: LOW ENERGY NEUTRAL ATOMS IN THE MAGNETOSPHERE

MOORE ET AL.: LOW ENERGY NEUTRAL ATOMS IN THE MAGNETOSPHERE

MOORE ET AL.: LOW ENERGY NEUTRAL ATOMS IN THE MAGNETOSPHERE

MOORE ET AL.: LOW ENERGY NEUTRAL ATOMS IN THE MAGNETOSPHERE

MOORE ET AL.: LOW ENERGY NEUTRAL ATOMS IN THE MAGNETOSPHERE

MOORE ET AL.: LOW ENERGY NEUTRAL ATOMS IN THE MAGNETOSPHERE